Multiscale Simulation as a Framework for the Enhanced Design of Nanodiamond-Polyethylenimine-based Gene Delivery

Hansung Kim[†‡], *Han Bin Man*[†‡], *Biswajit Saha*[¶], *Adrian M. Kopacz*[†], *One-Sun Lee*[¶], *George C. Schatz*[¶*], *Dean Ho*[§*], *and Wing Kam Liu*[†⊥*]

[†]Department of Mechanical Engineering, Robert R. McCormick School of Engineering and Applied Science, Northwestern University, Evanston, Illinois 60208 USA; [¶]Department of Chemistry, Northwestern University, Evanston, Illinois 60208 USA; [§]Division of Oral Biology and Medicine, Division of Advanced Prosthodontics, The Jane and Jerry Weintraub Center for Reconstructive Biotechnology, UCLA School of Dentistry, California NanoSystems Institute, and Jonsson Comprehensive Cancer Center, University of California, Los Angeles, Los Angeles, California 90095, USA; [⊥]Distinguished World Class University Professor, School of Mechanical Engineering, Sungkyunkwan University, Suwon, Kyonggi-do, Republic of Korea; [‡]These authors contributed equally to this work.

[*]Address correspondence to: w-liu@northwestern.edu, dean.ho@ucla.edu, schatz@chem.northwestern.edu

KEYWORDS : Gene delivery, Nanodiamond, Multiscale simulation, Molecular dynamics, Density function theory.

Supporting Information

SI Materials and Methods

Quantum Simulation DFTB is an approximate density functional theory (DFT) method based on the tight binding approximation. It uses an optimized minimal linear combination of atomic orbitals (LCAO) Slater-type valence-only basis set in combination with a two-center approximation for the Hamiltonian matrix elements. Several benchmark calculations with first principles density functional theory (DFT)[1-3] and Møller−Plesset second order perturbation theory[4] have been performed on systems consisting of carbon atoms to test DFTB, and this has established DFTB as a computationally inexpensive yet reliable quantum chemical level of theory for carbon clusters. Explicit consideration of electronic structure, such as π-conjugation, aromaticity, and delocalization stabilization, is important for carbon cluster systems and is well described by DFTB. In the SCC-DFTB formalism, self-consistency is included at the level of Mulliken charges.[5] A 4.1 nm ND contains 5795 carbon atoms (C_{5795}), so full optimization of this system is not feasible with standard self-consistent-charge (SCC)-DFTB methods. The non-charge-consistent (NCC) approximation of DFTB, which is a good approximation for carbon only systems, was adopted to obtain the optimized geometry of the ND since SCC-DFTB was not feasible in this case.[6-7] This approximation was a suitable compromise between accuracy and computational rigor since this carbon-only system exhibits negligible charge transfer between atoms.[6-7] ND surface charge, an essential attribute for modeling interactions with small molecules, was

then determined for the NCC-derived structure using the more rigorous SCC-DFTB. The NDs considered here are shaped like truncated octahedrons, with 8 hexagonal surfaces and 6 square surfaces with [111] and [100] facet planes respectively (Figure 2A). It has been shown that truncated octahedral NDs are more thermodynamically stable than alternative shapes.[8] The core carbon atoms exhibit sp3 hybridization whereas most surface carbon atoms exhibit sp2 hybridization. Mulliken charges were calculated using SCC-DFTB to obtain the ND surface charge distribution (Figure 2D).

ND Characterization NDs (Nanocarbon Research Institute, Japan) were diluted in pure water to a concentration of 20 mg/ml and underwent ultrasonication overnight (Fisher Scientific). NDs were adjusted to a concentration of 4 mg/ml prior to titration. A 50 ml solution of NDs was titrated with 0.01M NaOH (Sigma Aldrich) added at 0.5 ml increments. The pH of the solution was recorded prior to each addition using a pH meter (Mettler Toledo).

Calculating pKa of NDs

$$pH = pK_a - \log\left(\frac{[HA]}{[A^-]}\right)$$

According to the Henderson-Hasselbalch relation (above), the pH at the half-equivalence point is equal to the pKa of the solution being titrated. When the log term is zero, in the Henderson-Hasselbalch equation (above), the pH of the solution is equal to the pKa of the solution. Thus, when the concentration of the acid equals to the concentration of the conjugate base, or at the half equivalence point, the log term becomes zero and the pH equals the pKa. As NDs are dispersed in water (4.5<pH<5),

protons dissociate from the functional groups on their surfaces. A sharp rise in pH indicates the end point, or equivalence point, of the titration, where the titrant is close to neutralizing all of the conjugate base in solution. The half-equivalence point is halfway between the start of the titration and the equivalence point.

pKa and Ionization of ND Surface. While the ND surface may have complex speciation (multiple interacting ionizable sites), we used the measured pKa value to effectively model the pH dependence of the fraction of surface charges on the functionalized NDs. This fraction may be obtained from the Henderson-Hasselbalch equation as follows.

$$pK_a = pH + log\left(\frac{[1-x]}{[x]}\right) \qquad (1)$$

$$x = \frac{N_{charged}}{N_{total}} = \frac{1}{1 + 10^{pk_a - pH}}$$

$$N_{charged} = \frac{N_{total}}{1 + 10^{pk_a - pH}}$$

In. Eq. 1. x = fraction of ionized sites, $N_{charged}$ = the number of ionized sites on the ND surface, N_{total} = the number of ionizable sites on the ND surface

At every ionized site, a charge of -1e is assigned to that atom. These charges are combined with the surface charges determined from DFTB to obtain an overall charge that is used for our molecular dynamics studies. Notice that since the detailed surface structure of the ND is unknown, we have omitted carboxylate groups or other acidic groups in the model by lumping the acid and surface charges together. This approach was used previously[9] where it led to an accurate description of the binding of DOX to NDs.

Derivation of Equation 1

	$HA + H_2O \leftrightarrow H_3O^+ + A^-$			
Initial [mole/liter]:	**Q**			
Change [mole/liter]:	**-R**		**+R**	**+R**
Final [mole/liter]:	**Q-R**		**+R**	**+R**

HA: Acid, A^- : Conjugate base

$$pK_a = pH + \log\left(\frac{[HA]}{[A^-]}\right) \rightarrow pK_a = pH + \log\left(\frac{[Q-R]}{[R]}\right) \rightarrow pH + \log\left(\frac{[1-x]}{[x]}\right)$$

$\frac{R}{Q}$: Fraction of ionized site

MD Simulations of siRNA: The atomic structure of the C-myc siRNA (Fig. S6) (6.75 nm in length, 1.8 nm in diameter) was generated by the Nucleic Acid Builder (NAB) in Amber software (Amber 11)[10-11] using the exact sequence provided by the supplier of the siRNA (AACAGAAAUGUCCUGAGCAAU). The AMBER force field (ff10) was used to simulate the C-Myc siRNA.[10] The distribution of PEI, siRNA, water, and counterions in the simulation domain was determined using PACKMOL software.[12]

Preparation of ND-PEI Complexes NDs were dispersed and diluted to a working concentration of 5 mg/ml. After ultrasonication, NDs underwent sterilization *via* liquid autoclave. To prepare ND-PEI complexes, NDs were combined with PEI (800 Da, Sigma

Aldrich) at various mixing ratios to a final volume of 1 ml and a final ND concentration of 1 mg/ml. After 1 min of vortexing, samples were incubated (15 min, room temperature) to allow for complexing. Samples underwent centrifugation (1 h, 14000 rpm) to pellet complexed ND-PEI, leaving unbound PEI in the supernatant. After excess PEI was removed, the pellet of ND-PEI was resuspended in water using probe sonication (Fisher Scientific) yielding a clear solution. Three wash steps were performed to remove all excess PEI. ND-PEI complexes were produced and remained stable for >1 month (4^{O} C).

Characterization of PEI loading onto NDs 0.2 ml of supernatant was reacted with 0.5 ml of 0.150 mg/ml $CuSO_4 \cdot 5H_2O$ (Sigma Aldrich) to quantify the PEI concentration. Since the PEI concentration, after reaction with $CuSO_4$, is linearly correlated with absorbance at 285 nm[13], a standard curve was generated (0.05 - 1 mg/ml) in order for the PEI concentration in the supernatant to be quantified. The amount of unbound PEI was subtracted from initial PEI concentration to determine PEI loading.

Characterization of siRNA loading onto ND-PEI

0.0875 mg of ND-PEI (ND weight, 1mg/ml ND:PEI) was complexed with siRNA, with water added to adjust final mixing volume to 225 µl. Human C-Myc siRNA (AACAGAAAUGUCCUGAGCAAU) (Santa Cruz Biotechnology) at a 10 µM concentration was complexed with ND-PEI at various mixing ratios (ND:siRNA w/w). After gentle vortexing, the ND-PEI was allowed to incubate with siRNA (15 min, room temp) before centrifugation (30 min, 14000 rpm). Once ND-PEI-siRNA particles were pelleted, the supernatant was collected to determine unbound siRNA. 20 µl of supernatant from each sample was reacted with 200 µl of reagent from a Quant-iT RNA Assay Kit

(Life Technologies) before fluorescent readings (ex. 644 nm, em. 673nm) were performed. A standard curve was constructed (0.01 – 5 μM) and results compared against it to quantify RNA content. The amount of unbound siRNA was subtracted from initial siRNA concentration to determine siRNA loading.

Supporting Figures

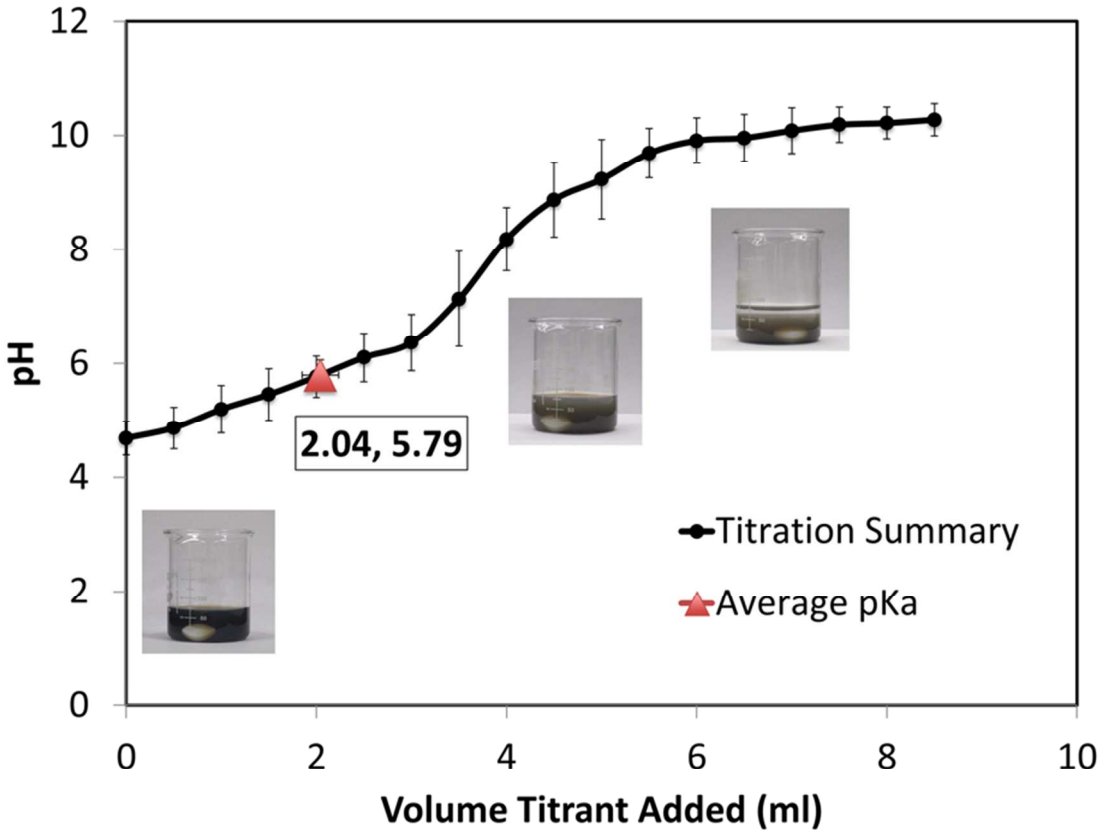

Fig. S1 A graph of the titration of ~50 ml of NDs at a concentration of 4 mg/ml titrated with 0.01M NaOH at 0.5 ml increments. There is a steep rise in pH at around 3.5 ml, indicating the onset of the equivalence point (midpoint of the rise). The pH at the half equivalence point (mean = 5.79), depicted by the red triangular marker (mean = 2.04 ml titrant), is the pKa of the ND solution. All results shown are mean + SE (standard error) over 3 titration trials (n = 3). The images show the state of titration at the beginning of the titration (far left), near the equivalence point (middle), and at the end-point (far right).

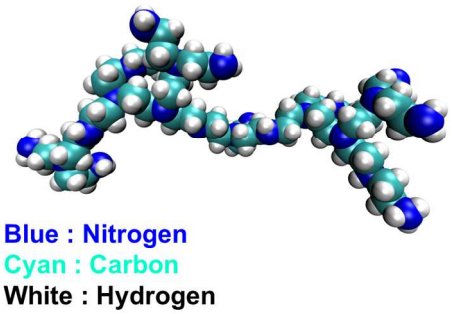

Fig. S2 Atomic model of branched PEI (800 Da) structure that is used to form the ND-PEI complexes. The atomic structure measures 3.5 nm in length, 1.6 nm in height, and 1.0 nm in width.

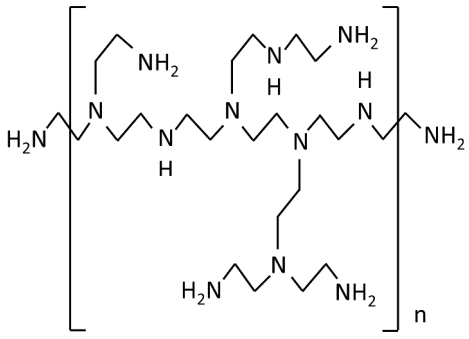

Fig. S3 The chemical formula of PEI 800.

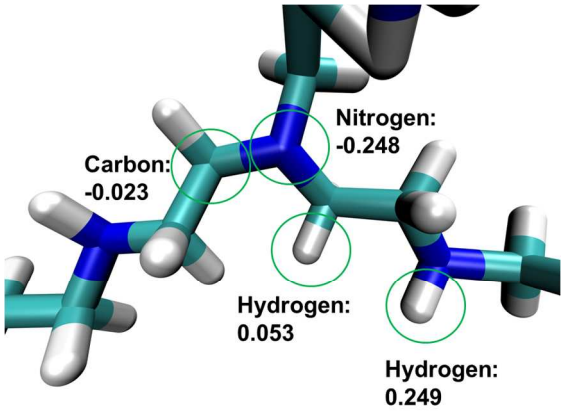

Fig. S4 The charge assignment of the 4 types of atomic configurations in PEI 800.

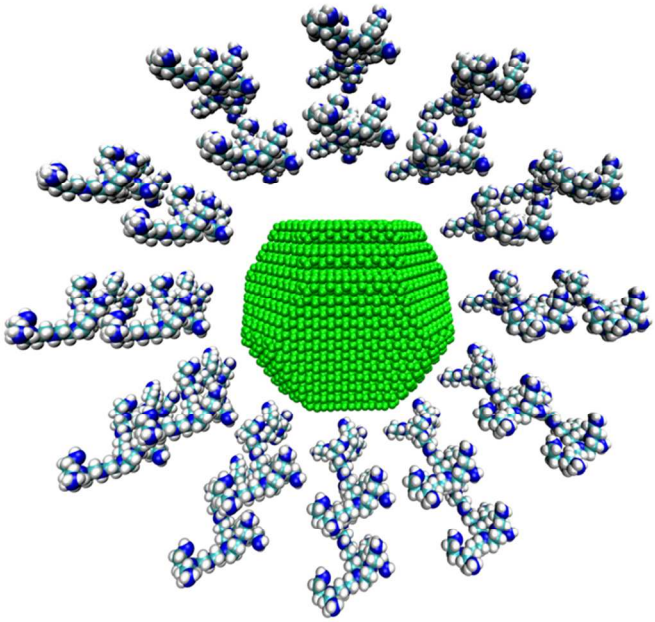

Fig. S5. Initial structure of a ND with 24 PEIs surrounding the particle, corresponding to Fig. 4A and 4B. PEIs were placed around both functionalized and non-functionalized NDs to test the importance of surface functionalization to PEI binding. The PEIs were placed in the same initial positions for both types of NDs to ensure that the comparison of the two results is valid.

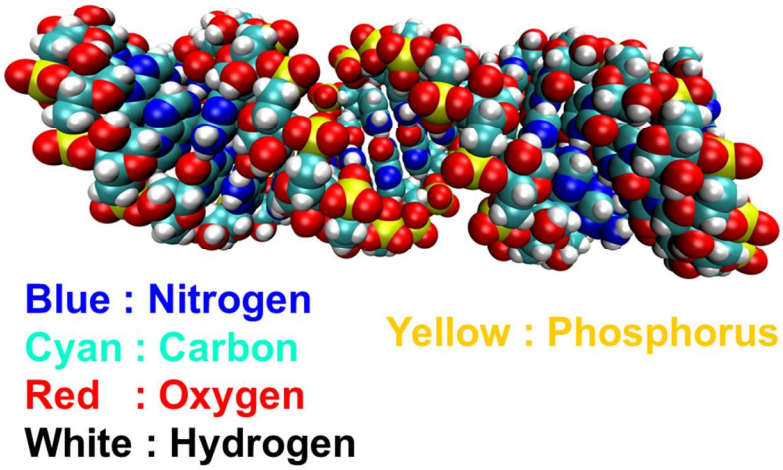

Fig. S6. Atomic model of a C-myc siRNA strand structure (6.75 nm in length, 1.8 nm in diameter)

Supporting Tables

Table S1. The detailed results of PEI loading for various mixing ratios (1:25 to 1:300, ND:PEI ratio by weight) for both simulations and experiments. Simulation results used 1 ND in a simulation volume of 1000 nm^3, and the number of PEI placed in this region was adjusted to match the different mixing ratios. The final loading values (mean ± SE) are averaged over 10 trials (n=10). Experimental results used 1 mg of NDs in a total mixing volume of 1 ml, and the weight of PEI complexed with NDs were adjusted to match the different mixing ratios. The final loading values (mean ± SE) are averaged over 3 trials (n=3).

ND:PEI Mixing Ratio (w/w)	Simulation Results				
	NDs in Simulation Domain (number)	PEI (number)	Water Molecules (number)	PEI Bound to one ND (number)	
				Average	Standard Deviation
1:25	1	15	31000	14	0.95
1:50	1	30	31000	24	1.6
1:100	1	60	29300	40	3.36
1:200	1	120	27000	60	3.81
1:300	1	180	25000	62	2.64
	Experimental Results				
	Total Volume (ml)	ND (mg)	PEI (mg)	PEI bound per mg of ND (mg)	
				Average	Standard Deviation
1:25	1	1	25	0.55	0.02
1:50	1	1	50	1.97	0.12
1:100	1	1	100	3.57	0.27
1:200	1	1	200	5.53	0.09
1:300	1	1	300	5.34	0.12

Table S2: The detailed results for siRNA loading for various mixing ratios (1:0.05 to 1:0.20, ND:siRNA ratio by weight) for both simulations and experiments. Simulation results used 1 ND-PEI (1 ND with 57 PEI, 1:200 ND:PEI mixing ratio) in a 140 Å cubic simulation box, and the number of siRNA placed in this region was adjusted to match the different mixing ratios. The final loading values (mean ± SE) are averaged over 10 trials (n=10). Experimental results used 0.0875 mg (ND weight) of ND-PEI in a total mixing volume of 0.225 ml, and the mgs of siRNA complexed with ND-PEI were adjusted to match the different mixing ratios. The final loading values (mean ± SE) are averaged over 3 trials (n=3).

ND:siRNA Mixing Ratio (w/w)	Simulation Results					
	NDs in Simulation Domain (number)	PEI (number)	siRNA (number)	siRNA Bound to one ND-PEI (number)		
				Average	Standard Deviation	Fraction of Initial siRNA Bound
1:0.05	1	57	2	2	0	1
1:0.067	1	57	3	3	0	1
1:0.10	1	57	4	4	0	1
1:0.13	1	57	6	5	0.44	0.87
1:0.20	1	57	9	7	0.71	0.78
	Experimental Results					
	Total Volume (ml)	ND:PEI (mg, ND weight)	siRNA (μM)	siRNA bound (μM)		
				Average	Standard Deviation	Fraction of Initial siRNA Bound
1:0.05	0.225	0.0875	1.33	1.25	0.062	0.94
1:0.067	0.225	0.0875	1.77	1.65	0.050	0.93
1:0.10	0.225	0.0875	2.66	2.54	0.088	0.95
1:0.13	0.225	0.0875	3.54	3.12	0.033	0.88
1:0.20	0.225	0.0875	5.33	4.18	0.271	0.78

REFERENCES

(1) Elstner, M.; Porezag, D.; Jungnickel, G.; Elsner, J.; Haugk, M.; Frauenheim, T.; Suhai, S.; Seifert, G., Self-Consistent-Charge Density-Functional Tight-Binding Method for Simulations of Complex Materials Properties. *Phys Rev B* **1998,** *58*, 7260-7268.

(2) Porezag, D.; Frauenheim, T.; Kohler, T.; Seifert, G.; Kaschner, R., Construction of Tight-Binding-Like Potentials on the Basis of Density-Functional Theory - Application to Carbon. *Phys. Rev.B* **1995,** *51*, 12947-12957.

(3) Zheng, G. S.; Irle, S.; Morokuma, K., Performance of the DFTB Method in Comparison to DFT and Semiempirical Methods for Geometries and Energies of C-20-C-86 Fullerene Isomers. *Chem. Phys. Lett.* **2005,** *412*, 210-216.

(4) Dolgonos, G. A.; Peslherbe, G. H., Calculations of the C-2 Fragmentation Energies of Higher Fullerenes C-80 and C-82. *J. Mol. Model.* **2007,** *13*, 981-986.

(5) Frauenheim, T.; Seifert, G.; Elstner, M.; Niehaus, T.; Kohler, C.; Amkreutz, M.; Sternberg, M.; Hajnal, Z.; Di Carlo, A.; Suhai, S., Atomistic Simulations of Complex Materials: Ground-State and Excited-State Properties. *J. Phys.: Condens. Matter* **2002,** *14*, 3015-3047.

(6) Saha, B.; Shindo, S.; Irle, S.; Morokuma, K., Quantum Chemical Molecular Dynamics Simulations of Dynamic Fullerene Self-Assembly in Benzene Combustion. *Acs Nano* **2009,** *3*, 2241-2257.

(7) Saha, B.; Irle, S.; Morokuma, K., Hot Giant Fullerenes Eject and Capture C-2 Molecules: Qm/Md Simulations with Constant Density. *J Phys Chem C* **2011,** *115*, 22707-22716.

(8) Barnard, A. S.; Russo, S. P.; Snook, I. K., Structural Relaxation and Relative Stability of Nanodiamond Morphologies. *Diam. Relat. Mater.* **2003,** *12*, 1867-1872.

(9) Adnan, A.; Lam, R.; Chen, H.; Lee, J.; Schaffer, D. J.; Barnard, A. S.; Schatz, G. C.; Ho, D.; Liu, W. K., Atomistic Simulation and Measurement of Ph Dependent Cancer Therapeutic Interactions with Nanodiamond Carrier. *Mol. Pharm.* **2010,** *8*, 368-374.

(10) Case, D. A.; Darden, T. A.; Cheatham, T. E.; III, C. L. S.; Wang, J.; Duke, R. E.; R.Luo; Walker, R. C.; Zhang, W.; Merz, K. M.*, et al.*, Amber 11. University of California: San Francisco, 2010.

(11) Macke, T. J.; Case, D. A., Modeling Unusual Nucleic Acid Structures. *Acs Sym Ser* **1998,** *682*, 379-393.

(12) Martinez, L.; Andrade, R.; Birgin, E. G.; Martinez, J. M., Packmol: A Package for Building Initial Configurations for Molecular Dynamics Simulations. *J Comput Chem* **2009,** *30*, 2157-2164.

(13) Ungaro, F.; De Rosa, G.; Miro, A.; Quaglia, F., Spectrophotometric Determination of Polyethylenimine in the Presence of an Oligonucleotide for the Characterization of Controlled Release Formulations. *J. Pharmaceut. Biomed.* **2003,** *31*, 143-149.